# Testing Cosmogonic Models with Gravitational Lensing

Joachim Wambsganss, Renyue Cen, Jeremiah P. Ostriker, Edwin L. Turner

**Gravitational lensing provides a strict test of cosmogonic models because it is directly sensitive to mass inhomogeneities. Detailed numerical propagation of light rays through a universe that has a distribution of inhomogeneities derived from the standard CDM (cold dark matter) scenario, with the aid of massive, fully nonlinear computer simulations, was used to test the model. It predicts that more widely split quasar images should have been seen than were actually found. These and other inconsistencies rule out the Cosmic Background Explorer (COBE)–normalized CDM model with density parameter $\Omega = 1$ and the Hubble constant $(H_0) = 50$ kilometers second$^{-1}$ megaparsec$^{-1}$; but variants of this model might be constructed, which could pass the stringent tests provided by strong gravitational lensing.**

Gravitational lensing directly measures fluctuations in the gravitational potential along lines of sight to distant objects. In contrast, the conventional tools for comparing theories with observations rely on either galaxy density or velocity information whose quality unavoidably suffers from uncertainties with regard to the density or velocity bias of galaxies in comparison with the underlying mass distribution; this hampers our attempts to understand the more fundamental questions about mass evolution and distribution. Thus gravitational lensing provides a powerful independent test of cosmogonic models (*1*, *2*). Each model for the development of cosmogonic structure [such as the HDM (hot dark matter) or CDM scenario] has at least one free parameter: the amplitude of the density (or gravitational potential) Fourier power spectrum. In light of COBE observations (*3*) of temperature fluctuations in the microwave background light, however, that parameter is fixed by the ($\pm$15%) determination on a scale of 5° to 10° in the linear regime.

Each model is defined by the Fourier power spectrum $P(k)$ of density fluctuations as a function of wave number $k$. Although the shape of the function $P(k)$ is determined by the model, the amplitude was previously unknown. Now that its amplitude has been determined, the density fluctuations on all scales can be specified for a specific model. Moreover, a precise determination of the potential fluctuation on any scale provides a test; any single conflict between the theory and reality can falsify the former. The greatest leverage is obtained for tests made on scales as far as possible from the COBE measurements. The reason is that all models have an assumed power spectrum that passes through the COBE normalization point at the very large comoving scales ($\lambda \approx 1000$ Mpc) fixed by that measurement. Because the slope of the power spectrum is a primary model-dependent feature, the maximum variations among models typically occur at the smallest scales. Thus, one looks for tests at scales as small as possible, but they should not be so small as to be influenced greatly by the difficulty in modeling the physics of the gaseous, baryonic components ($\leq$10 kpc). Thus, critical tests are best made on scales 0.01 Mpc $< r <$ 1 Mpc. Our purpose is to use gravitational lensing from matter distributions on these scales to test the standard CDM scenario.

The model simulated here is the CDM scenario with $\Omega = 1$, $\lambda = 0$, and $H_0 = 100h = 50$ km s$^{-1}$ Mpc$^{-1}$ that currently is taken as standard. It is the simplest model that satisfies the philosophical requirement for a flat universe with $\Omega = 1$ (that is, no cosmological constant $\lambda$). Normalization, taken from the COBE first year results (*3*), corresponds to root-mean-square mass fluctuations in a sphere ($8h^{-1}$ Mpc) close to unity, specifically $\sigma_8 = 1.05$ (*4*). To allow for the existence of very large-scale waves, we first ran a large-size box ($L = 400h^{-1}$ Mpc) with $500^3 = 10^{8.1}$ cells and $250^3 = 10^{7.2}$ particles. In addition, to have detailed small-scale information we reran a total of 10 independent simulations with $L = 5h^{-1}$ Mpc, which had $500^3 = 10^{8.1}$ cells and $250^3 = 10^{7.2}$ particles. This gave us the required large dynamic range of scales from 400 Mpc to 10 kpc. Knowing the distribution of overdensities on the scale of $5h^{-1}$ Mpc from the large simulation, we can convolve the small and large scale runs statistically to produce simulated sheets or screens of matter spaced $5h^{-1}$ Mpc apart between the observer at $z = 0$ and a putative galaxy or quasar in the source plane at $z = z_S$.

A large number of independent runs (10 runs were simulated) is required so that identical structures do not repeat along a line of sight. The details of the convolution method and tests of it by means of a high-resolution, large-dynamic-range P$^3$M simulation provided by Bertschinger and Gelb (*5*) are being determined. This method is statistically reliable for describing structures in the range 30 kpc $< \Delta Lh <$ 1.2 Mpc, which corresponds roughly to splitting angles 5 arc sec $< \theta <$ 200 arc sec. On these scales, we expect that dark matter dominates over baryons, so that a dark matter–only simulation is approximately valid.

We presented a very preliminary attack on this problem in a previous paper (*2*). In that work, no ray tracing was done. We simply checked whether or not mass accu-

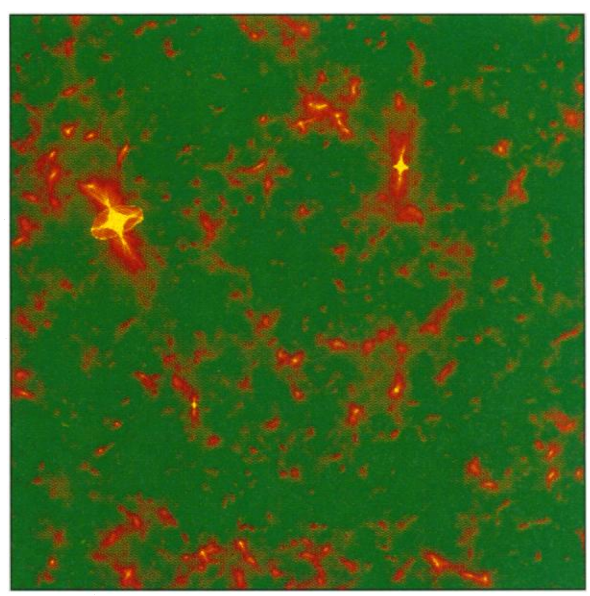

**Fig. 1.** Example of the magnification caused by the gravitational lens action of a CDM, $\Omega = 1$ universe for a source plane at $z_S = 3.0$. The size of the field is about 5.7$^2$ arc min$^2$. The colors indicate increases in magnification, as they change from green through red to yellow. Yellow indicates magnification by more than one magnitude. The yellow regions with the sharp boundaries (caustics) indicate regions of multiple imaging. The diamond-shaped structure on the left side that is surrounded by a yellow ellipse indicates the caustic structure of a clump of dense matter at a redshift $z = 0.201$, whereas the isolated diamond in the top right originates from a mass concentration at $z = 0.426$. Both of these regions would contain multiple quasars, or giant luminous arcs, if a quasar or an extended galaxy were sited at these locations.

J. Wambsganss, Astrophysikalisches Institut Potsdam, An der Sternwarte 16, 14482 Potsdam, Germany.
R. Cen, J. P. Ostriker, E. L. Turner, Princeton University Observatory, Princeton, NJ 08544, USA.

mulations were greater than the critical level (6) at which multiple imaging will occur. In addition to applying what we believe is the much better method used here, we modified and improved the convolution algorithm over the one previously adopted (2).

In principle, we now know the density distributions, according to the specified model, everywhere along the line of sight between us and the quasar. We can shoot rays through this line of sight to see how they are bent and how the inhomogeneous mass distribution alters the images of distant objects. As a numerical convenience, we represent the matter in each cube as if it were concentrated as a surface density on a screen at the midplane of the cube, and then we group the screens further. Specifically, in our ray-tracing routine, we use the multiplane lens equations (7) and speed the calculation of deflection angles by use of the hierarchical tree code (8), typically with 200 to 300 (grouped) screens used for each ray tracing. Amplitude on the image plane is given simply by the differential area within a bundle of rays, compared with what it would have been had the propagation been through a universe that contains smoothly distributed matter. Figure 1 shows the amplitude distribution for sources of a redshift $z_S = 3$. When a given region on the source plane is reached by rays in separate disconnected regions of the image plane, the observer would see multiple images of the same object.

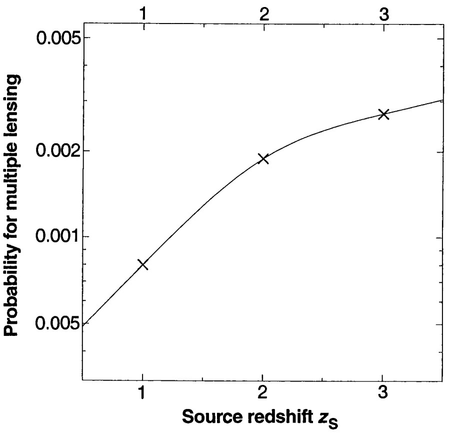


**Fig. 2.** Probability of a splitting with separation of images greater than 5 arc sec and magnitude difference less than 1.5 as a function of source redshift.

We have computed the distribution of magnifications for single and multiply imaged point sources as a function of $z_S$, multiplicity of images, and distribution of angular splittings. In addition, for extended sources (mock galaxies), we have computed the expected shape distortions, frequency, and properties of the giant arcs that would be seen when the sources are lensed by intervening clusters (9) of galaxies. Figure 2 shows the probability of a splitting with separation of images greater than 5 arc sec and magnitude difference less than 1.5 as a function of source redshift. These numbers were chosen so that the multiple images would be distinct, and we can be fairly sure that observers would not have missed them. In fact, amplification bias (6, 10, 11) will increase the probabilities over those shown in Fig. 2 by a significant amount. Splittings larger than 5 arc sec should be common (when several thousand quasars have been examined), if this cosmogonic model were correct.

Probably the single most revealing statistic is the distribution of image separations expected for multiple sources, as shown in Fig. 3 for $z_S = 1$, 2, and 3. Notice that very large splittings should be the rule. Also revealing is the distribution of expected lens redshifts, as shown in Fig. 4. The lenses themselves should be close enough to be seen by ground-based observers in almost all cases. On this issue, the recent observation (12) of a lens candidate for the double quasar QSO2345+007 is extremely relevant. The separation of the two images is 7.06 arc sec, the quasar redshift is $z_S = 2.15$, and the putative lens is at $z_L = 1.49$. We see from Fig. 4 that although a separation of 7 arc sec can be produced in the CDM model, the probability that the lens is as far away as $z = 1.49$ is very small (2%), because of the relatively late formation of structure in this model. In open cosmological models, structure formation occurs earlier.

It appears that all three of these results, shown in Figs. 2 to 4, are seriously in conflict with the existing observations. In particular, we find that the standard CDM model predicts that 0.0007 of all lines of sight to $z_S = 1$, 0.0014 of all lines of sight to $z_S = 2$, and 0.0020 of those to $z_S = 3$ will be multiply imaged with angular splittings $\geq 10''$ and with amplification ratios of less than 4. Surveys (12–18) and occasional serendipitous discoveries have revealed 27 confirmed or possible multiply imaged quasi-stellar objects (QSOs) according to a recent compilation (19). Detailed analysis (20, 21) of the most statistically useful of these surveys (14–16) yields a lensing rate in the vicinity of a few tenths of one percent to one percent, consistent with the CDM predictions quoted above after allowance is made for plausible magnification biases (22). However, as shown in Fig. 3, all observed QSO lens systems have image splittings of less than 10 arc sec and most have splittings less than 5 arc sec.

**Fig. 3 (left).** Multiple-lensing probability distribution as a function of image separations for sources at $z_S = 1$, 2, and 3. Also shown as a long dashed curve is the observed distribution (13). **Fig. 4 (right).** Integrated lensing probability distribution as a function of expected lens redshift. The symbol X indicates the recent observation (12) of a lens candidate for the double quasar QSO2345+007.

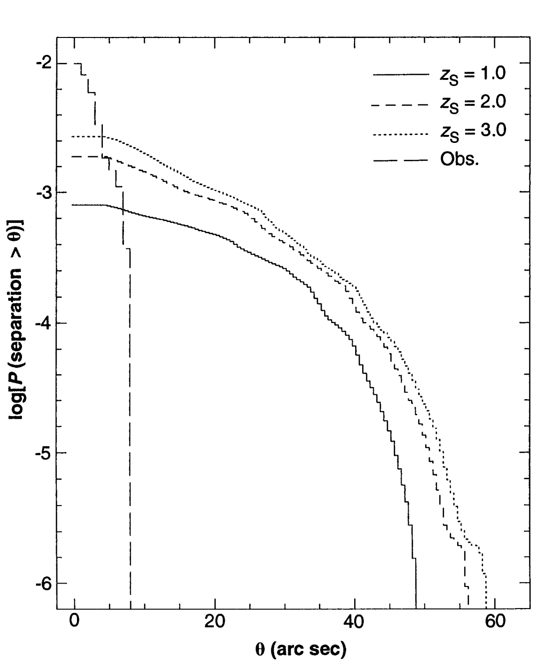


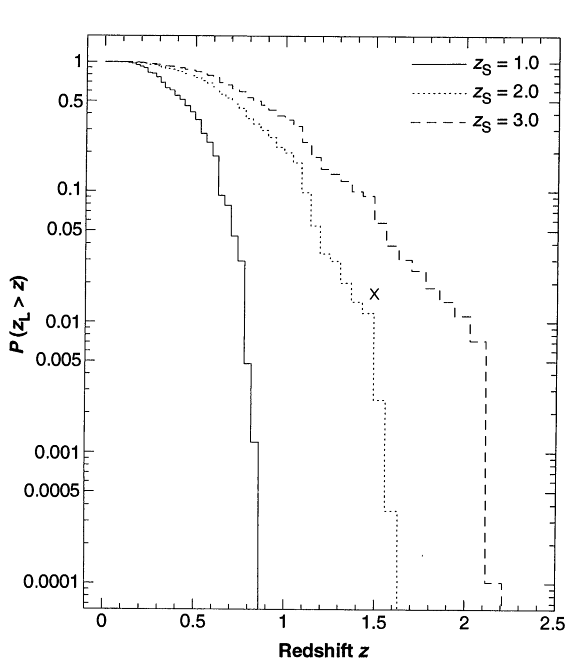

These data sharply contradict, and thus falsify the model. No escape by appeal to observational selection seems possible because the large-splitting, modest brightness ratio systems predicted by that model typically would be much easier to detect and recognize than those 27 that actually have been found. Could the observational selection effects and magnification bias not treated in this paper alter our conclusions? A recent treatment of this problem by Kochanek (*23*) carefully allowed for these effects (but did not perform the detailed numerical simulations we report here). From this work, we conclude that these effects [which were treated in an approximate fashion in our previous work (*2*)] would not alter our conclusions.

The failing of the model investigated is not presented as an entirely new result, but as a new and more robust manifestation of a previously recognized problem; namely, the excessively deep potential wells produced by the dark matter component in COBE-normalized standard CDM (*24–26*). These excessively deep potential wells lead to excess galactic pairwise velocity dispersions and to the predicted, excessive rate of large-splitting lensing events. The virtue of the lensing test is that it is independent of other tests and is not subject to the same caveats concerning bias of galaxies with respect to dark matter.

Are there variant models that would not fail these tests? Many alternative models have been considered or reconsidered in recent years. All of these add extra parameters such as allowance for a nonstandard spectrum shape, for other components of matter (such as massive neutrinos), or for less matter than is assumed in the flat ($\Omega = 1$) models. The simplest change that one can make in the standard scenario is to reduce the density of the clumped material in the universe, because the large number of large mass concentrations is what produces the overabundance of large splittings. Thus, a lower value of $\Omega$ clearly is useful (this also increases the computed age of the universe), but it would be premature to argue that our results by themselves indicate $\Omega < 1$, for many other properties of the scenario (such as temperature of the dark matter and shape of the power spectrum) contribute to lensing properties. However, the directness of gravitational lensing as a test for the growth of inhomogeneities, coupled with the rapidly increasing power of computers and numerical algorithms, makes us optimistic that calculations of the type about which we report here should become a major tool for testing and discriminating among competing cosmological scenarios.

### REFERENCES AND NOTES


1. R. Narayan and S. D. M. White, *Mon. Not. R. Astron. Soc.* **231**, 97 (1988).
2. R. Cen, J. R. Gott, J. P. Ostriker, E. L. Turner, *Astrophys. J.* **423**, 1 (1994).
3. G. F. Smoot, *et al.*, *ibid.* **396**, L1 (1992).
4. G. Efstathiou, J. R. Bond, S. D. M. White, *Mon. Not. R. Astron. Soc.* **258**, 1 (1992).
5. E. Bertschinger and J. Gelb, *Astrophys. J.* **436**, 467 (1994).
6. E. L. Turner, J. P. Ostriker, J. R. Gott III, *ibid.* **284**, 1 (1984).
7. P. Schneider, J. Ehlers, E. E. Falco, *Gravitational Lensing* (Springer-Verlag, Berlin, 1992).
8. J. Wambsganss, thesis, Max-Planck-Institute for Physics and Astrophysics, Munich (1990).
9. B. Fort and Y. Mellier, *Astron. Astrophys. Rev.* **5**, 239 (1994).
10. E. L. Turner, *Astrophys. J.* **243**, L135 (1980).
11. R. Narayan and S. Wallington, in *Gravitational Lenses in the Universe*, J. Surdej *et al.*, Eds. (University of Liège, Liège, Belgium, 1993), p. 217.
12. P. Fischer, J. A. Tyson, G. M. Bernstein, P. Guhathakurta, *Astrophys. J.*, in press.
13. J. Surdej *et al.*, *Astron. J.* **105**, 2064 (1993).
14. D. Maoz *et al.*, *Astrophys. J.* **409**, 28 (1993).
15. H. K. C. Yee, A. V. Fillipenko, D. Tang, *Astron. J.* **105**, 7 (1993).
16. D. Crampton, R. D. McClure, J. M. Fletcher, *Astrophys. J.* **392**, 23 (1992).
17. A. R. Patnaik, I. W. Browne, D. Walsh, F. H. Chaffee, C. B. Folts, *Mon. Not. R. Astron. Soc.* **259**, 1 (1992).
18. J. N. Hewitt *et al.*, *Lect. Notes Phys.* **330**, 147 (1989).
19. J. Surdej and G. Soucail, *Proceedings of the 31st Liège International Astrophysical Colloquium* (University of Liège Liège, Belgium, 1993), p. 205.
20. D. Maoz and H.-W. Rix, *Astrophys. J.* **416**, 425 (1993).
21. C. S. Kochanek, *ibid.* **417**, 438 (1993); *ibid.* **419**, 12 (1993).
22. M. Fukugita and E. L. Turner, *Mon. Not. R. Astron. Soc.* **253**, 99 (1991).
23. C. S. Kochanek, Harvard-Smithsonian CfA preprint 3985 (1994).
24. M. Davis, G. Efstathiou, C. S. Frenk, S. D. M. White, *Nature* **356**, 489 (1992).
25. N. A. Bahcall and R. Cen, *Astrophys. J.* **398**, L81 (1992).
26. J. P. Ostriker, *Annu. Rev. Astron. Astrophys.* **31**, 689 (1993).


27. We thank J. R. Gott, C. S. Kochanek, and P. Schneider for useful discussions and the National Center for Supercomputing Applications for our use of the Convex-3880 supercomputer. We also gratefully acknowledge the financial support of NASA grants NAGW-2448 and NAGW-2173 and NSF grants AST92-08103 and HPCC ASC-9318185.

2 November 1994; accepted 31 January 1995


# Imaging the Pore Structure of Geomaterials


J. T. Fredrich,* B. Menéndez,† T.-F. Wong



**Laser scanning confocal microscopy can be used to image the pore structure of geologic materials in three dimensions at a resolution of 200 nanometers. The technique involves impregnation of the void space with an epoxy doped with a fluorochrome whose fluorescent wavelength matches the excitation wavelength. Optical sections with a thickness of less than 1 micrometer can be sliced from thick polished sections and combined to produce three-dimensional reconstructions. Application of the technique to rocks with porosities from 1 to 20 percent reveals the geometric complexity of the pore space. The technique can also be applied to other brittle solids such as ceramics.**


The pore structure of rocks is both varied and complex: Crystalline rocks are dominated by microcracks (*1*), whereas sedimentary rocks typically contain voids in a variety of shapes, including nodal pores situated at grain vertices and sheetlike throats (microcracks) along two-grain boundaries (*2*). Physical rock properties such as permeability, electrical resistivity, seismic velocity, elastic moduli, and strength are affected not only by the porosity but also by the pore size distribution and connectivity (*3*). The compressive failure of rock involves damage accumulation (*4*), which significantly modifies the pore geometry.

Statistical descriptions of the pore space can be inferred indirectly from mercury injection, small-angle scattering, and adsorption analyses (*5*); however, direct observational methods permit quantification of diverse parameters including porosity, specific surface area, pore size and shape distribution, connectivity, surface roughness, and grain contact area. Conventional imaging technologies, such as optical light microscopy and scanning electron microscopy, rely on the analysis of polished planar sections. However, damage, in the form of widened cracks or pores and eradicated fine structure, may be induced during preparation and obscure analysis. Although ion milling has been proposed (*6*) to etch away the upper layer of damaged material, the technique is time consuming and problems can arise that are due to differential thinning rates in polymineralic rocks (*7*). A more important limitation (*8*) is that conventional techniques are confined to a two-dimensional (2D) view of a three-dimensional (3D) structure. Although pore casts can be prepared for qualitative study (*9*), destructive serial sectioning is necessary for quantitative characterization. Conventional serial sectioning techniques (*10*) are deficient in that


J. T. Fredrich, Geomechanics Department 6117, Sandia National Laboratories, Albuquerque, New Mexico 87185-0751, USA.
B. Menéndez and T.-F. Wong, Department of Earth and Space Sciences, State University of New York, Stony Brook, New York 11794-2100, USA.

*To whom correspondence should be addressed.
†Present address: Institut de Physique du Globe de Strasbourg, 67084 Strasbourg Cedex, France.